IEEE Access
Multidisciplinary | Rapid Review | Open Access Journal

Received September 13, 2020, accepted September 16, 2020, date of publication September 21, 2020,
date of current version October 1, 2020.

Digital Object Identifier 10.1109/ACCESS.2020.3025357

Vibration Control of Truck Cabins With the Adaptive Vectorial Backstepping Design of Electromagnetic Active Suspension System

SINAN BASARAN[1], (Member, IEEE), AND MURAT BASARAN[2]
[1]Department of Mechanical Engineering, Bilecik Seyh Edebali University, 11230 Bilecik, Turkey
[2]Vocational School of Transportation, Eskisehir Technical University, 26140 Eskisehir, Turkey

Corresponding author: Sinan Basaran (sinan.basaran@bilecik.edu.tr)

ABSTRACT The active suspension system is an important equipment that isolates the vibrations that may come from outside in a land vehicle. In heavy vehicles, the active suspension system can be used to dampen vibrations in the driver's cabin. The electromagnetic actuator is used as an active element in suspension system. Traditionally, the use of active suspension systems is mainly on automobiles and the studies related to heavy vehicles like trucks lack enough interest. In this study, dynamic modeling of a three-axle heavy vehicle cabin is performed with a half-car approach and it is aimed to suppress the disruptive effects coming from the road with active electromagnetic actuators. Lyapunov based backstepping control design is expressed in vectorial form for the heavy vehicle system, which is a multi-input multi-output system. To demonstrate the performance of the designed controller, a comparison has been made for the active and passive states for the truck cabin suspension system. The main feature of the applied control method is that it does not require knowing the actuator parameters, the adaptive term can handle the estimate of the actuator parameter. The stability of the proposed system has been proven via Lyapunov based arguments and given simulation works. The results obtained are important to suppress vibration, consequently, decreases the vibration exposure for truck drivers in terms of occupational health and safety aspects.

INDEX TERMS Adaptive backstepping control, truck cabin suspension system, truck modeling.

I. INTRODUCTION

Driving comfort, handling, and driver and passenger safety can be listed as important aspects of studies related to land vehicle systems. Long-distance truck drivers experience various health problems by being exposed to long-term vibrations. The exposure of truck drivers to whole-body vibration (WBV) causes physical and mental fatigue as well as creates serious risks in terms of occupational safety. Therefore, active-controlled suspension systems are applied to reduce the amount of the vibration that the driver will be exposed to. Although the tires and the main suspension system are essential anti-vibration elements in a vehicle, cabin suspension systems to be encountered in trucks. Active control in the truck cabin is an easier solution than to interfere with the entire truck's suspension system. There are three different suspension designs in the literature: active, semi-active, and passive. Preliminary work and optimization design are important in passive suspension design [1]–[6]. In passive suspension systems, the basic elements are springs and dampers, and there is no active control force. Suspension systems with active control are referred to as semi-active and active suspension systems. The semi-active suspension system controls the damping force of the shock absorber in response to input from the continuously varying road surfaces [7]–[10]. The main role of a semi-active suspension system is to change the cross-sectional area that put together the two chambers of the damper's piston acquirement performance from a shock absorber equipment [11]. The popular forms of the semi-active suspension systems are with electrorheological (ER) and magnetorheological (MR) fluids in the control of shock absorbers [12], [13]. Yildiz and Sivrioglu designed a new constrained adaptive backstepping control approach for road excitation suppression of their quarter-car experimental suspension setup equipped with a magnetorheological absorber [14]. Nonlinear dynamic analysis of a semi-active suspension system with MR damper investigated by Zhang and friends in their study [15]. The active

The associate editor coordinating the review of this manuscript and approving it for publication was Jinquan Xu.

This work is licensed under a Creative Commons Attribution 4.0 License. For more information, see https://creativecommons.org/licenses/by/4.0/

control of the suspension system is another type of vibration suspension structure popular in both academic research and industrial applications. The advantages of an active force producing equipment have already been worked in various research [16]–[24]. Active suspension force-producing mechanism is maintained by active power sources such as compressors, hydraulic pumps, etc. Conventional implementation of active suspensions has been accompanied with microprocessors and associated with the computer. For the investigations of active suspension structure and vehicle dynamics, different types of vehicle models are constructed by several researchers [25]–[27]. Three different main dynamic models are used in suspension control systems. These are quarter-car vehicle [28]–[30], half-car vehicle [31]–[33], and full-car vehicle models [34]–[37]. In general, the left and the right sides of the vehicles are symmetrical, so the mathematical model of the vehicle can be customizable as a half-car model. The half-car model can express both vertical and pitch displacements of the vehicle. In the truck model, it is possible to examine the dynamics of both the chassis and the cabin by applying the half-car model.

During modeling of heavy vehicles, cabin suspension systems other than the main suspension system are also considered. When we look at the literature, there are vibration suspension actuator applications in the seat systems to prevent vibrations encountered by heavy vehicles [38], [39]. D. Ning et. al. designed and built an electromagnetic interface for a heavy-duty vehicle seat suspension to reduce the vibration transferred to driver bodies [40]. Also, D. Ning *et al.* in their another study, proposed and built an energy regenerative seat suspension and worked on a semi-active controller for vibration control [41]. Current studies have been focused directly on the driver's seat as an anti-vibration element. However, the importance of the cabin suspension systems, in which the driver and passengers together and directly affects the vehicle dynamics, has been highlighted in only a few studies. As reported from Soliman's work, the main suspension system in trucks stands out for its handling and maneuverability [42]. But suspension systems in the truck cabins are designed for comfort and occupational health and safety (OHS) of the driver. Mayhew and Quinlan reported that there have been few studies related to the OHS effects associated with economic pressure in transport [43]. Therefore, OHS has always been an issue for truck drivers. Nitti and Santis were studied for assessment and prediction of WBV exposure in transport truck drivers and emphasized the importance of developing cabin suspension systems [44]. Caffaro and friends have investigated whether an active cabin suspension system fitted on a telehandler was effective in reducing WBV or not, and in improving the comfort in their study [45]. Johnson and friends worked to show the WBV exposure differences between the conventional and cab-over design flatbed trucks, and they found that the conventional design performed better in exposures [46]. Deprez and friends studied to generate a method for optimization in suspension systems with a global optimization method. They have tested their proposed design procedure on a hydropneumatic cabin suspension system of off-road machinery [47]. The economic impact of the comfort that concerns the driver in the truck is of secondary importance. To prevent this situation, Nakano *et al.* have proposed the idea of self-powered active control system to the cabin suspension of a heavy-duty truck [48]. They used the regenerated energy from the damper element in the main suspension system to obtain the necessary source for active suspension of the cabin of the truck. Employees of the magnetorheological damper manufacturer company have stated that they have reduced WBV that were harmful to drivers in a heavy vehicle cabin system using MR damper in their study [49]. Elmadany presented a paper of the active suspension system of a tractor-semitrailer cabin for randomly profiled roads [50]. He performed a Linear Quadratic Gaussian (LQG) control theory for the proposed design.

When the current active suspension studies are inspected, it is seen that the mainstream trend is on automobiles and the studies related to heavy vehicles like trucks are lack of enough interest. In the literature, the importance of the design of an active suspension system for truck cabins investigated by many researchers, but there is a lack of control design, which is the most important process of active control systems. In this research, a three-axle heavy vehicle truck model cabin suspension control design is introduced. The dynamic equations of the truck obtained by the half-car model approach. It is aimed to suppress the vibrations due to different road conditions. The results obtained are important to suppress vibration, consequently, decreases an important risk for truck drivers in terms of occupational health and safety. The electromagnetic actuator is used as the active control element of the cabin suspension system. The superior aspects of the electromagnetic actuator like increase in efficiency, improved dynamic behavior, stability improvement, precise force control, and dual operation mode, which are advantageous compared to active elements such as hydraulics and pneumatics, and its application to the suspension system is given in the study of Gysen *et al.* [51]. Studies which utilize the electromagnetic actuators in automobile suspension systems are mentioned in references [52]–[54]. In these studies, vehicle suspension systems have been investigated, with bring to the fore on linear motor or electromagnetic actuator models. However, electromagnetic actuator designs are not emphasized in truck cabin suspension systems. The parameters of the truck model used in this study are taken from [55]. In control systems, the adaptive backstepping method is developed to perform tracking control or regulation control for many different types of systems [56]. In the proposed active cabin suspension system, Lyapunov based vectorial adaptive backstepping algorithm is selected for the controller scheme. Besides, the adaptive control approach is applied to the designed controller for the actuator dynamics of the system. Recently, Lyapunov type adaptive controller has been preferred by many researchers as an important control algorithm for control systems [57], [58]. Adaptive control is a

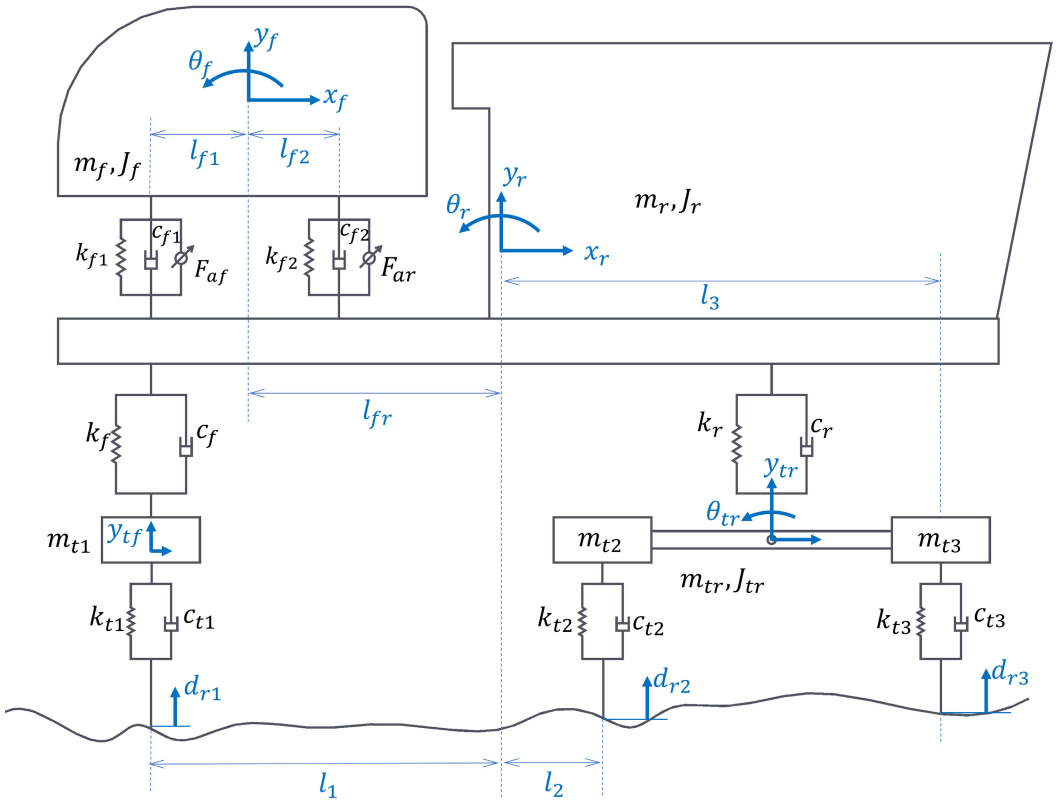

FIGURE 1. Representative view of the truck with an active cabin suspension system.

technique used to control various systems whose parameters are unknown [59]–[62]. Active disturbance rejection method is also applicable in adaptive controller design, considering unmodeled disturbances, as well as system parametric uncertainties [63], [64]. In the proposed system, the motor constant of the electromagnetic actuator is treated as uncertain but estimated by the controller update rule and the control algorithm is implemented in a vectorial form [65].

This paper is organized as follows: In section two, seven degree of freedom (7-DOF) truck's mathematical model is presented. In section three, the details of Lyapunov based adaptive vectorial backstepping control design are given. The responses and simulation results of the active cabin suspension system for the road bump input and the random road input cases are given in section four. In the following sections, simulation results and the concluding remarks are given.

Notations: In this paper, $\mathcal{R}$ denotes the set of real numbers, superscript "$\mathcal{R}^n$" denotes the n-dimensional space, boldface capital letters represent the matrices, eye$(\cdot)$ represents the identity matrix, $diag\{\cdots\}$ represents the diagonal matrix, the transpose of the matrix $\boldsymbol{A}$ is denoted by $\boldsymbol{A}^{\boldsymbol{T}}$, and, the first and second derivatives are denoted by superscripts "." and ".." respectively.

II. MATHEMATICAL MODELING OF A TRUCK

The balanced suspension system has been applied to enhance the axle load in trucks and in order to demonstrate vibration characteristics of trucks, it is essential to build up a model [66]. The truck dynamics with three axles with balanced suspension can be modeled with 7-DOF considering the half-car approach. Fig.1 shows the representative view of the truck with an active cabin suspension system. Here, the suspension structure used on the rear axles in the truck is a balanced type suspension structure. All separate tires are considered as stiffness and damping element in the mathematical model of the system.System states can be taken as y_f, θ_f, y_r, θ_r, y_{tf}, y_{tr}, and θ_{tr}. Here y_f and θ_f represents the vertical displacement of the truck cabin and the angular displacement of the cabin center of mass. The truck body vertical displacement and the angular displacement is given by y_r and θ_r respectively. Front axle vertical displacement is given by y_{tf}. And finally; y_{tr} and θ_{tr} represents the vertical displacement and the angular displacement of the tandem balanced suspension. The first equation of motion is the vertical displacement for the truck cabin is given below:

$$m_f \ddot{y}_f + F_{f1} + F_{f2} = F_{af} + F_{ar} \tag{1}$$

where; F_{f1} is the front suspension force between truck cabin and body and F_{f2} is the rear suspension force between the truck cabin and body as defined below.

$$\begin{aligned} F_{f1} = {} & k_{f1}\left(y_f - y_r + \theta_r\left(l_{fr} + l_{f1}\right) - \theta_f l_{f1}\right) \\ & + c_{f1}\left(\dot{y}_f - \dot{y}_r + \dot{\theta}_r\left(l_{fr} + l_{f1}\right) - \dot{\theta}_f l_{f1}\right) \end{aligned} \tag{2}$$

$$\begin{aligned} F_{f2} = {} & k_{f2}\left(y_f - y_r + \theta_r\left(l_{fr} - l_{f2}\right) + \theta_f l_{f2}\right) \\ & + c_{f2}\left(\dot{y}_f - \dot{y}_r + \dot{\theta}_r\left(l_{fr} - l_{f2}\right) + \theta_f l_{f2}\right) \end{aligned} \tag{3}$$

The control force of the electromagnetic actuator is defined by F_{af} and F_{ar} for the front and rear location of the truck cabin respectively. The detailed investigation of the electromagnetic actuator is worked by Gysen *et al.* in references [22], [51]. The electromagnetic force equations can be defined as below;

$$F_{af} = \mu i_f \tag{4}$$
$$F_{ar} = \mu i_r \tag{5}$$

where i_f and i_r represent the control currents of the actuator at the front and rear location of the truck cabin and, μ is the motor constant of the actuators. The second equation of motion is obtained for angular displacement for the truck cabin is given below:

$$J_f \ddot{\theta}_f - F_{f1} l_{f1} + F_{f2} l_{f2} = -l_{f1} F_{af} + l_{f2} F_{ar} \tag{6}$$

The truck body vertical and angular displacement differential equations are given in (7) and (8) respectively.

$$m_r \ddot{y}_r - F_{f1} - F_{f2} - F_f - F_r = -F_{af} - F_{ar} \tag{7}$$

$$J_r \ddot{\theta}_r + F_{f1}\left(l_{fr} + l_{f1}\right) + F_{f2}\left(l_{fr} - l_{f2}\right) + F_f l_1 - F_r\left(\frac{l_2 + l_3}{2}\right) = F_{af}\left(l_{fr} + l_{f1}\right) + F_{ar}\left(l_{fr} - l_{f2}\right) \tag{8}$$

here; F_f is the front suspension force and F_f is the rear suspension force as defined below:

$$F_f = k_f\left(y_{tf} - y_r + \theta_r l_1\right) + c_f\left(\dot{y}_{tf} - \dot{y}_r + \dot{\theta}_r l_1\right) \tag{9}$$
$$F_r = k_r\left(y_{tr} - y_r - \frac{\theta_r\left(l_2 + l_3\right)}{2}\right) + c_r\left(\dot{y}_{tr} - \dot{y}_r - \frac{\dot{\theta}_r\left(l_2 + l_3\right)}{2}\right) \tag{10}$$

The front location suspension tire vertical direction and balanced suspension vertical direction equations of motions are given (11) and (12) respectively,

$$m_{t1} \ddot{y}_{tf} + F_f + F_{t1} = 0 \tag{11}$$
$$\left(m_{tr} + m_{t2} + m_{t3}\right) \ddot{y}_{tr} + F_r + F_{t2} + F_{t3} = 0 \tag{12}$$

here; F_{t1}, F_{t2}, and F_{t3} are the front, middle and rear tire suspension force equations as defined below:

$$F_{t1} = k_{t1}\left(y_{tf} - d_{r1}\right) + c_{t1}\left(\dot{y}_{tf} - \dot{d}_{r1}\right) \tag{13}$$
$$F_{t2} = k_{t2}\left(y_{tr} - \frac{\theta_{tr}\left(l_3 - l_2\right)}{2} - d_{r2}\right) + c_{t2}\left(\dot{y}_{tr} - \frac{\dot{\theta}_{tr}\left(l_3 - l_2\right)}{2} - \dot{d}_{r2}\right) \tag{14}$$
$$F_{t3} = k_{t3}\left(y_{tr} + \frac{\theta_{tr}\left(l_3 - l_2\right)}{2} - d_{r3}\right) + c_{t3}\left(\dot{y}_{tr} + \frac{\dot{\theta}_{tr}\left(l_3 - l_2\right)}{2} - \dot{d}_{r3}\right) \tag{15}$$

Finally, the differential equation of motion for the rear balanced suspension rod angular direction is as follows:

$$\left(J_{tr} + \frac{\left(m_{t2} + m_{t3}\right)\left(l_3 - l_2\right)^2}{4}\right) \ddot{\theta}_{tr} - \frac{F_{t2}\left(l_3 - l_2\right)}{2} + \frac{F_{t3}\left(l_3 - l_2\right)}{2} = 0 \tag{16}$$

The displacement input signals for tires, resulting from the road profile are d_{r1}, d_{r2}, and d_{r3}. It is assumed that the tires are not separated on the road during the movement of the truck. The compact form of the seven equations of motion of the trucks' with an active cabin suspension system can be written in matrix form to use in controller design:

$$\boldsymbol{M}\ddot{\boldsymbol{Y}} + \boldsymbol{C}\dot{\boldsymbol{Y}} + \boldsymbol{K}\boldsymbol{Y} = \mu \boldsymbol{F}\boldsymbol{u} + \boldsymbol{K_t}\boldsymbol{d} + \boldsymbol{C_t}\dot{\boldsymbol{d}} \tag{17}$$

where $\boldsymbol{Y} = \begin{bmatrix} y_f & \theta_f & y_r & \theta_r & y_{tf} & y_{tr} & \theta_{tr} \end{bmatrix}^T$ and $\boldsymbol{u} = \begin{bmatrix} i_f & i_r \end{bmatrix}^T$, are the displacement and electromagnetic actuator control current vectors respectively. Also, $\boldsymbol{M} \in \mathcal{R}^{7\times7}$ is the positive-definite system mass matrix, $\boldsymbol{C} \in \mathcal{R}^{7\times7}$ is the system damping matrix, $\boldsymbol{K} \in \mathcal{R}^{7\times7}$ is the system stiffness matrix and finally $\boldsymbol{F} \in \mathcal{R}^{7\times2}$ represents the control current input matrix. In this equation, the motor constant parameter for the electromagnetic actuator is denoted by $\mu \in \mathcal{R}^1$. It should be noted that the motor constant parameter is adapted since the actual value of it is unknown, consequently, this value is taken out of the matrix $\boldsymbol{F}$ as a multiplier. The disruptive effects coming from the road affecting the tires are shown with the vector $\boldsymbol{d} = \begin{bmatrix} d_{r1} & d_{r2} & d_{r3} \end{bmatrix}^T$, for the front, middle and, the rear tires, respectively. The tires' stiffness and damping values are collected in the $\boldsymbol{K_t} \in \mathcal{R}^{7\times3}$ and $\boldsymbol{C_t} \in \mathcal{R}^{7\times3}$ matrices, respectively. The parameters of the system dynamics equations of the 7-DOF truck system are given in Table 1.

III. LYAPUNOV BASED ADAPTIVE VECTORIAL BACKSTEPPING CONTROL DESIGN

The position tracking error vector $\boldsymbol{e}(t) \in \mathcal{R}^{7\times1}$ and its time derivative $\dot{\boldsymbol{e}}(t) \in \mathcal{R}^{7\times1}$ are defined as follows:

$$\boldsymbol{e} = \boldsymbol{Y} - \boldsymbol{Y_d} \tag{18}$$
$$\dot{\boldsymbol{e}} = \dot{\boldsymbol{Y}} - \dot{\boldsymbol{Y}}_{\boldsymbol{d}} \tag{19}$$

where $\boldsymbol{Y_d(t)} \in \mathcal{R}^{7\times1}$ is the desired trajectory of the system states. The first step of the proposed controller is defining the virtual control signal:

$$\dot{\boldsymbol{Y}} = \boldsymbol{s} + \boldsymbol{\alpha} \tag{20}$$

where $\mathbf{s} \in \mathcal{R}^{7\times1}$ is a filtered tracking error dynamics and $\boldsymbol{\alpha}$ is stabilizing function which can be chosen as:

$$\boldsymbol{\alpha} = \dot{\boldsymbol{Y}}_{\boldsymbol{r}} \tag{21}$$
$$\dot{\boldsymbol{Y}}_{\boldsymbol{r}} = \dot{\boldsymbol{Y}}_{\boldsymbol{d}} - \boldsymbol{\Lambda e} \tag{22}$$

with the combination of the virtual control signal (20), stabilizing function (21) and arbitrary reference function $\dot{\boldsymbol{Y}}_{\boldsymbol{r}}(\boldsymbol{t}) \in \mathcal{R}^{7\times1}$ (22), the filtered tracking error can be written as follows:

$$\boldsymbol{s} = \dot{\boldsymbol{e}} + \boldsymbol{\Lambda e} \tag{23}$$

TABLE 1. Parameters of the truck suspension system.

Parameters	Symbol	Values
Mass of the truck cabin	m_f	557.5 kg
Mass of the truck body	m_r	11523 kg
Mass of the unsprung front suspension	m_{t1}	412 kg
Mass of the balanced type back suspension	$m_{t2} = m_{t3}$	676 kg
Mass of the balanced rod of the rear suspension	m_{tr}	177 kg
Moment of inertia of the truck cabin	J_f	1020 kg·m^2
Moment of inertia of the truck body	J_r	55502 kg·m^2
Moment of inertia of the balanced rod of the rear suspension	J_{tr}	351 kg·m^2
Cabin front and rear stiffness	$k_{f1} = k_{f2}$	36230 N/m
Front main suspension stiffness	k_f	251380 N/m
Rear main suspension stiffness	k_r	206400 N/m
Front tire stiffness	k_{t1}	1100000 N/m
Middle and rear tire stiffness	$k_{t2} = k_{t3}$	2200000 N/m
Cabin front and rear damping	$c_{f1} = c_{f2}$	3620 N·s/m
Front main suspension damping	c_f	50636 N·s/m
Rear main suspension damping	c_r	25320 N·s/m
Front tire damping	c_{t1}	3500 N·s/m
Middle and rear tire damping	$c_{t2} = c_{t3}$	7000 N·s/m
Distance from the front suspension to center of the mass of the truck	l_1	3.64 m
Distance from the middle tire to center of the mass of the truck	l_2	2.06 m
Distance from the back tire to center of the mass of the truck	l_3	3.36 m
Distance from the front cabin suspension to center of the mass of the cabin	l_{f1}	1.2 m
Distance from the back cabin suspension to center of the mass of the cabin	l_{f2}	1 m
Distance from the center of the mass of the cabin to the center of the mass of the truck	l_{fr}	2.8 m

where $\boldsymbol{\Lambda} \in \mathcal{R}^{7\times7}$ is a diagonal, positive-definite, control gain matrix. Implementation of the backstepping design can be done with the arrangement of the system equations (17), (22) and (23)

$$\boldsymbol{M\dot{s}} = \mu\boldsymbol{Fu} - \boldsymbol{M\ddot{Y}_r} - \boldsymbol{C\dot{Y}_r} - \boldsymbol{Cs} - \boldsymbol{KY} + \boldsymbol{K_t d} + \boldsymbol{C_t\dot{d}} \tag{24}$$

where μ is the electromagnetic motor parameter value. Since the parameter is constant but unknown, it is necessary to define the estimation to the adaptation of this term. Now consider $\hat{\mu}$, which is an estimate of unknown μ instead. Here $\tilde{\mu} \in \mathcal{R}^1$ is the estimation error can be defined as in (25).

$$\tilde{\mu} = \mu - \hat{\mu} \tag{25}$$

When we derivate (25) in order to use in Lyapunov control design, it is seen that the derivation is equal to $\dot{\tilde{\mu}} = -\dot{\hat{\mu}}$ since the μ value is constant. The next step of the proposed adaptive vectorial backstepping control design is defining the Lyapunov candidate function to achieve the globally exponential stability of the system;

$$V = \frac{1}{2}\boldsymbol{e}^T\boldsymbol{\Phi_P e} + \frac{1}{2}\boldsymbol{s}^T\boldsymbol{Ms} + \frac{1}{2\gamma}\tilde{\mu}^2 \tag{26}$$

where $\boldsymbol{\Phi_P} \in \mathcal{R}^{7\times7}$ is the controller tune matrix and $\gamma \in \mathcal{R}^1$ is the adaptation gain. Note that the candidate function was determined to include the vectorial and scalar expressions simultaneously, by considering the dimensional analysis. Taking the derivative of the Lyapunov function and making the necessary arrangement gives:

$$\dot{V} = -\boldsymbol{e}^T\boldsymbol{\Phi_P\Lambda e} + \boldsymbol{s}^T\boldsymbol{\Phi_P e} + \boldsymbol{s}^T\boldsymbol{M\dot{s}} + \dot{\tilde{\mu}}\frac{1}{\gamma}\tilde{\mu} \tag{27}$$

with the combination of (24), the derivative of the Lyapunov equation turns in (28).

$$\dot{V} = \boldsymbol{s}^T\left(\left[\tilde{\mu} + \hat{\mu}\right]\boldsymbol{Fu} - \boldsymbol{M\ddot{Y}_r} - \boldsymbol{C\dot{Y}_r} - \boldsymbol{Cs} - \boldsymbol{KY} + \boldsymbol{K_t d} + \boldsymbol{C_t\dot{d}} + \boldsymbol{\Phi_P e}\right) - \boldsymbol{e}^T\boldsymbol{\Phi_P\Lambda e} - \dot{\hat{\mu}}\frac{1}{\gamma}\tilde{\mu} \tag{28}$$

To deal with the estimated parameter, we need to eliminate the term $\boldsymbol{s}^T\tilde{\mu}\boldsymbol{Fu} - \dot{\hat{\mu}}\frac{1}{\gamma}\tilde{\mu}$. Therefore, the update rule of the motor constant parameter can be defined as in (29).

$$\dot{\hat{\mu}} = \gamma\boldsymbol{s}^T\boldsymbol{Fu} \tag{29}$$

When we rewrite the update rule (29) into the derivative of the Lyapunov equation (28) turns into (30).

$$\dot{V} = \boldsymbol{s}^T\left(\left[\hat{\mu}\right]\boldsymbol{Fu} - \boldsymbol{M\ddot{Y}_r} - \boldsymbol{C\dot{Y}_r} - \boldsymbol{KY} + \boldsymbol{K_t d} + \boldsymbol{C_t\dot{d}} - \boldsymbol{Cs} + \boldsymbol{\Phi_P e}\right) - \boldsymbol{e}^T\boldsymbol{\Phi_P\Lambda e} \tag{30}$$

From (30), the control law term can be derived as in (31),

$$\hat{\mu}\boldsymbol{Fu} = \boldsymbol{M\ddot{Y}_r} + \boldsymbol{C\dot{Y}_r} + \boldsymbol{KY} - \boldsymbol{K_t d} - \boldsymbol{C_t\dot{d}} - \boldsymbol{\Phi_P e} - \boldsymbol{\Phi_D s} \tag{31}$$

where $\boldsymbol{\Phi_D} \in \mathcal{R}^{7\times7}$ is the controller tune matrix. Note that the control current vector $\boldsymbol{u}$ obtained by the pseudo-inverse of the $\boldsymbol{F}$ given below.

$$\boldsymbol{F}^\dagger = (\boldsymbol{F}^T\boldsymbol{F})^{-1}\boldsymbol{F}^T \tag{32}$$

When the control signal inputs i_f and i_r are derived from (31), they should be divided with adapted μ value. The adaptation and control block algorithm scheme can be seen in Fig.2 in detail. If we put the control law signal (31) and the adaptation term in (29), the negative definite derivative of the Lyapunov function obtained as follows.

$$\dot{V} = -\boldsymbol{s}^T\left(\boldsymbol{C} + \boldsymbol{\Phi_D}\right)\boldsymbol{s} - \boldsymbol{e}^T\boldsymbol{\Phi_P\Lambda e} \tag{33}$$

Since V is positive definite and $\dot{V}$ is negative definite, and globally exponential stability is achieved according to the theorem given below:

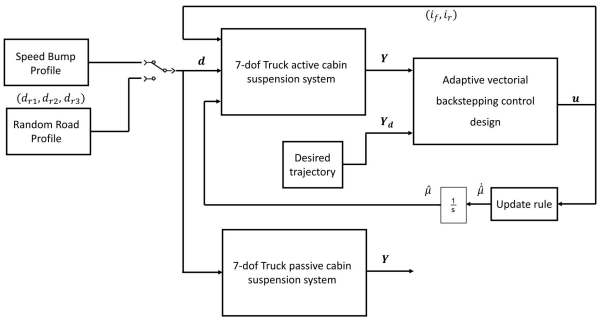

FIGURE 2. Schematic block diagram of the proposed controller design.

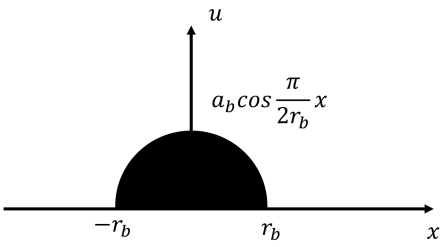

FIGURE 3. Schematic view of the road bump profile.

A. THEOREM

Let's assume that a function given in V and the $\alpha > 0$ is a constant. If V is positive definite and $\dot{V}(z) \leq -\alpha V(z)$ for all z, then there is an χ such that every trajectory of a function $\dot{x} = f(x)$ satisfying the given condition:

$$\|x(t)\| \leq \chi e^{-\alpha(t/2)} \|x(0)\| \tag{34}$$

then for any given system, the globally exponential stability is achieved [67].

IV. SIMULATION OF THE TRUCK WITH AN ACTIVE CABIN SUSPENSION SYSTEM

The proposed Lyapunov type adaptive backstepping controller for active truck cabin suspension system is tested in the Matlab-Simulink simulation environment for zero initial conditions of the system states. In simulations, disturbances coming from road surface taken as inputs in two different profiles, first one is for a road bump profile and the latter is random road profile, are realized with the control structure shown in Fig.2. Besides, the response of the proposed controller, which is designed by modeling in the passive system, where there is no active cabin control in the truck system with 7-DOF is also observed.

A. SPEED BUMP ROAD INPUT

For the simulation, first, the road bump profile which is frequently used in the testing of vehicle suspension systems' [68]–[70] but which is rarely used in truck systems [71] in literature is selected as an input. In Fig.3, the road bump profile which is used in modeling is depicted. Here,a_b shows the height of the bump and r_b shows the radius of the bump.

In the simulation, a time-varying input signal due to road bump is created and defined in (35-37) for the front, middle, and rear tire locations:

$$d_{r1} = \begin{cases} 0 \rightarrow & t < \dfrac{l_0 - r_b}{v_0} \\ \dfrac{a_b cos\pi\,(l_0 - v_0 t)}{2r_b} \rightarrow & \dfrac{l_0 - L_b}{v_0} \leq t \leq \dfrac{l_0 + r_b}{v_0} \\ 0 \rightarrow & t > \dfrac{l_0 + r_b}{v_0} \end{cases} \tag{35}$$

$$d_{r2} = \begin{cases} 0 \rightarrow & t < \dfrac{l_0 + l_1 + l_2 - r_b}{v_0} \\ \dfrac{a_b cos\pi\,(l_0 + l_1 + l_2 - v_0 t)}{2r_b} \rightarrow & \\ \dfrac{l_0 + l_1 + l_2 - r_b}{v_0} \leq t \leq \dfrac{l_0 + l_1 + l_2 + r_b}{v_0} & \\ 0 \rightarrow & t > \dfrac{l_0 + l_1 + l_2 + r_b}{v_0} \end{cases} \tag{36}$$

$$d_{r3} = \begin{cases} 0 \rightarrow & t < \dfrac{l_0 + l_1 + l_3 - r_b}{v_0} \\ \dfrac{a_b cos\pi\,(l_0 + l_1 + l_3 - v_0 t)}{2r_b} \rightarrow & \\ \dfrac{l_0 + l_1 + l_3 - r_b}{v_0} \leq t \leq \dfrac{l_0 + l_1 + l_3 + r_b}{v_0} & \\ 0 \rightarrow & t > \dfrac{l_0 + l_1 + l_3 + r_b}{v_0} \end{cases} \tag{37}$$

where t represent the time, v_0 is the truck speed, and finally l_0 is the horizontal distance for the bump center to the front tire center. This value depends on the truck speed which can be defined as in (38).

$$l_0 = 2v_0 + r_b \tag{38}$$

The speed of the truck is assumed to be constant and taken as $v_0 = 30$ km/h in simulation studies. Road bump inputs taken from the road for three of the wheels are given in Fig.4. The height and radius of the road bump is taken as $a_b = 0.1$ m, and $r_b = 0.3$ m respectively. The controller tuning gain matrices and adaptation rule gain for electromagnetic actuator constant are selected as below in simulation studies.

$$\mathbf{\Lambda} = \text{eye}(7) \times 10000 \tag{39}$$

$$\mathbf{\Phi_P} = \text{eye}(7) \times 10 \tag{40}$$

$$\mathbf{\Phi_D} = \text{diag}\left\{ 5e6 \quad 5e6 \quad 5e5 \quad 5e5 \quad 5e5 \quad 5e5 \quad 5e5 \right\} \tag{41}$$

$$\gamma = 0.5 \tag{42}$$

The axial and angular displacements of the truck cabin's center of mass are given respectively in Fig.5 and Fig.6. For comparison, results in the passive state where the active suspension is not issued are given with the dashed line in the figures. By utilization of the designed controller, it is observed that the amplitudes of the cabin displacement results are highly suppressed.

Besides, although the active control effect is only on the cabin in a 7-DOF truck system, Fig.7 is given to show how

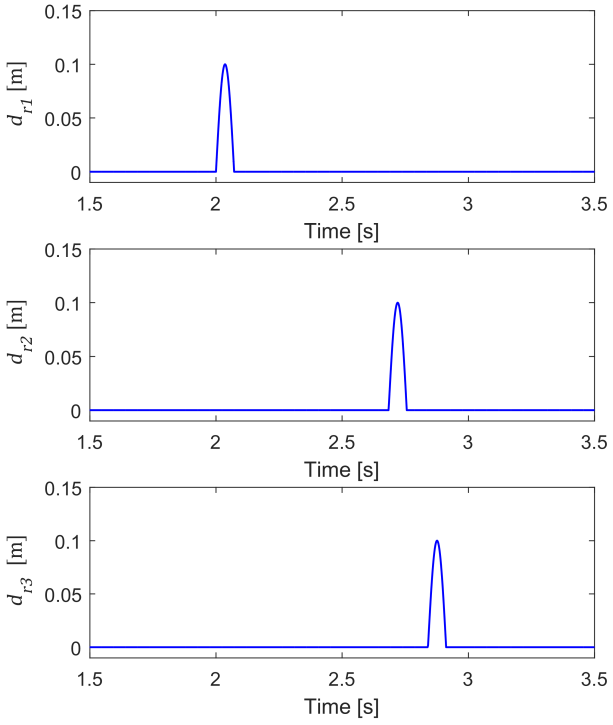

FIGURE 4. Speed bump road inputs for the front, middle, and rear tire locations.

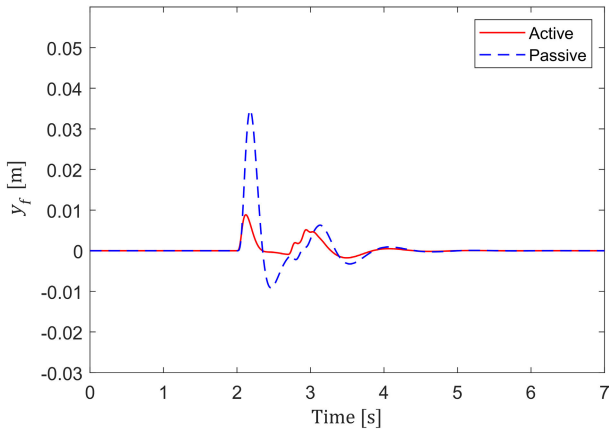

FIGURE 5. Cabin vertical displacement for the active and passive suspension system.

the road bump profile coming from the road surface affects other states of the system.

The control current results obtained with the use of electromagnetic actuators, which are the elements of the active suspension system, are given in Fig.8 for the front and in Fig.9 for the rear of the cabin.

Here, it is observed that the control current at the front location makes a peak from the ±15 A band. This value is at a level that can be obtained according to similar studies [22], [51]. The estimated value of the active electromagnetic actuator motor constant is given in Fig.10. By the

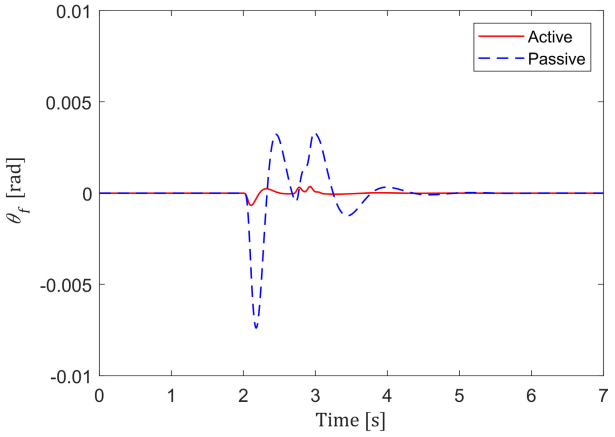

FIGURE 6. Cabin angular displacement for the active and passive suspension system.

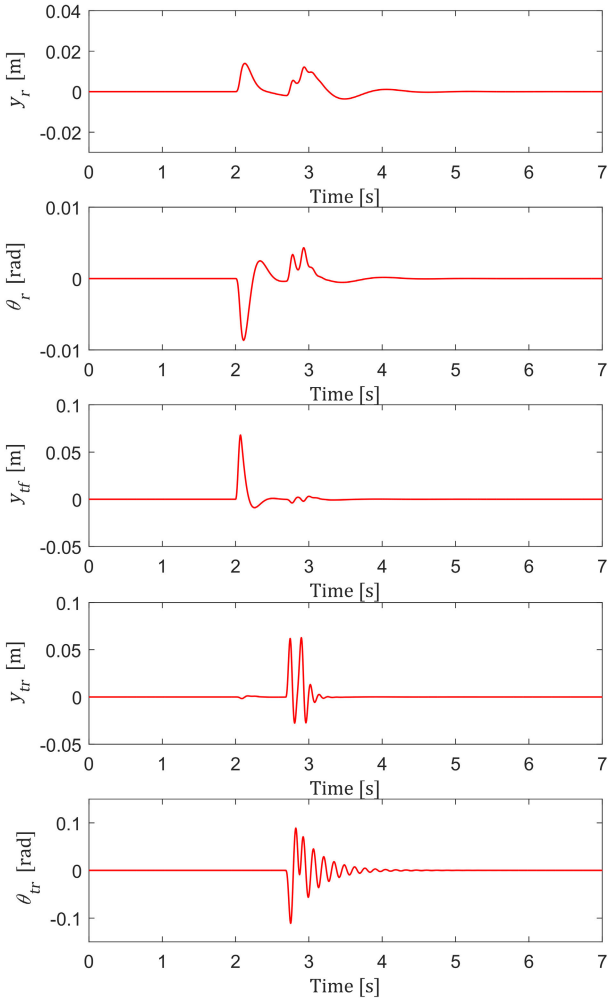

FIGURE 7. Remaining passive states where there is no effect of active control for road bump input.

utilization of the designed adaptive controller, it is seen that this value converges to a constant value in a short period in time. For the adaptation rule, $\mu(0)$=150 N/A was taken

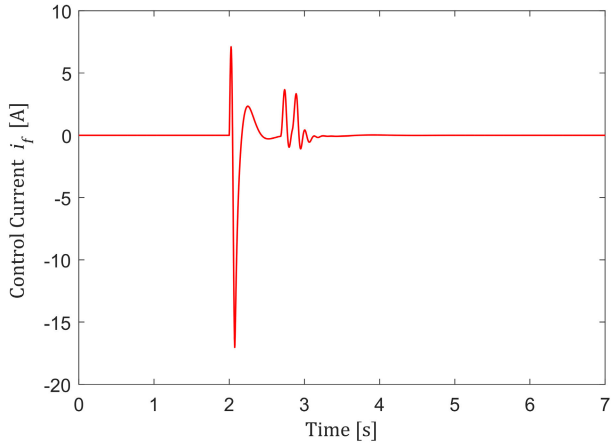

FIGURE 8. Control current for cabin actuator front location.

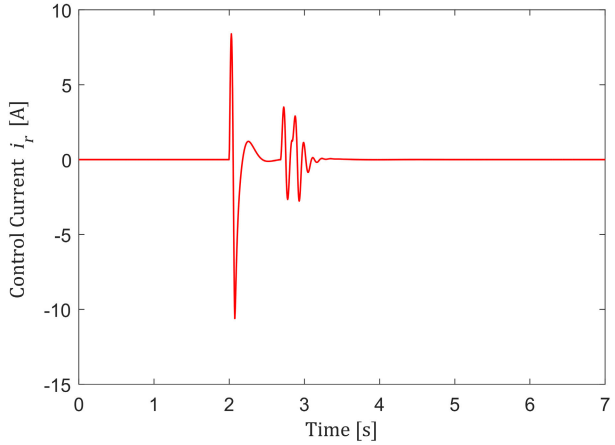

FIGURE 9. Control current for cabin actuator rear location.

as the initial condition. Note that here, the initial condition of the electromagnetic motor constant should be chosen as positive $\mu(0)>0$, since this adapted term is used as an denominator in (31), which is used to calculate control currents.

B. RANDOM ROAD INPUT

As the second simulation study, the cabin active suspension system was tested by representing the road surface disturbance characteristics by using random road input. To describe the stationary characteristics of road roughness, power spectral density (PSD) is one of the applicable tools.

Assuming a truck moving at a constant velocity v_0, the road surface roughness can be considered as a stationary process in the space domain and this approach is examined in many studies [72]–[74]. The road roughness can be defined using a white noise signal with a certain power spectral density. If a truck moves at a constant velocity, the road roughness can be expressed by the following equation

$$\dot{x}(t) + 2\pi v_0 n_0 x(t) = \sqrt{R(\Omega_0)\, v_0}\, w(t) \tag{43}$$

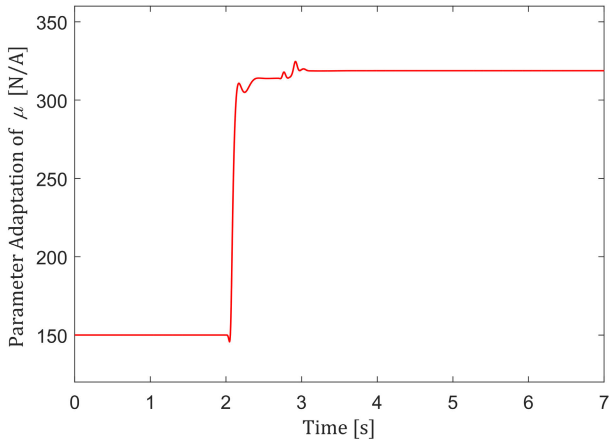

FIGURE 10. Parameter adaptation of the electromagnetic actuator constant.

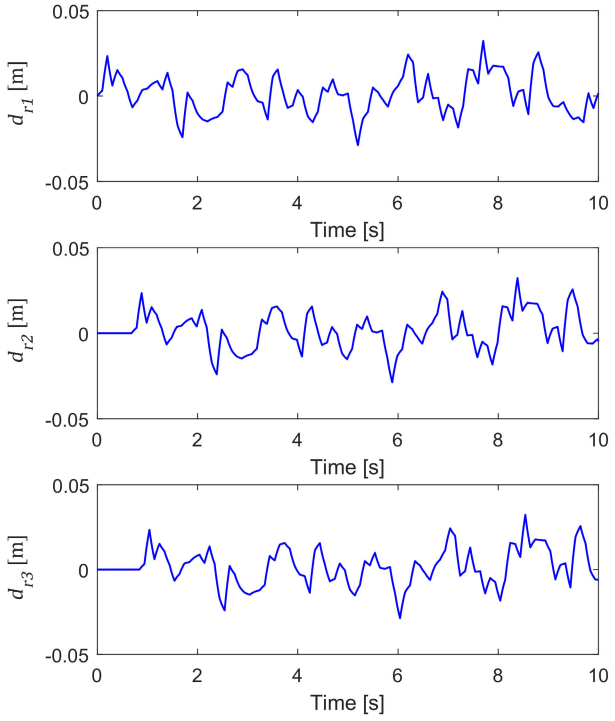

FIGURE 11. Random road input for three tire locations.

where $x(t)$ represents the road roughness, n_0 the reference spatial frequency, $R(\Omega_0)$ is the PSD of the road disturbance input and finally $w(t)$ is the waviness, which indicates the road's wavelengths. The waviness range is between $1.75 \leq w \leq 2.25$ and is taken usually $w = 2$ [72].

By applying the same control coefficients used in the previous section as in (39-42), system response is analyzed for random road input. In Fig.11, the applied random road input to the system is given for three of the tires. Note that for the given constant truck speed, since the required time to reach rough road surface is different for each of the tires, three different (d_{r1}, d_{r2}, d_{r3}) road inputs are created considering

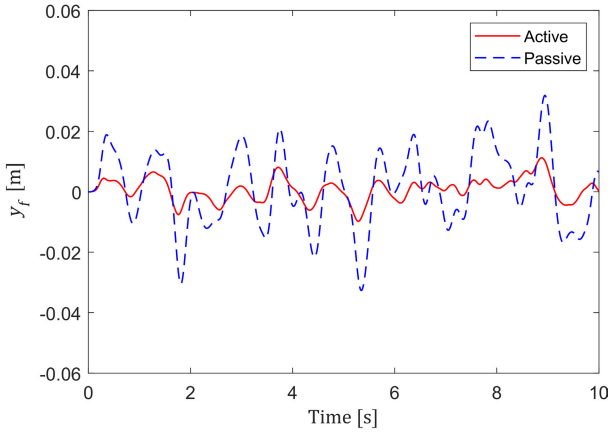

FIGURE 12. Cabin vertical displacement for active and passive suspension system for random road profile.

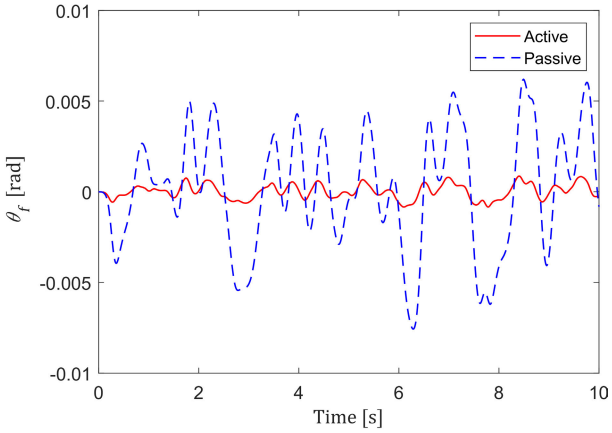

FIGURE 13. Cabin angular displacement for active and passive suspension system for random road profile.

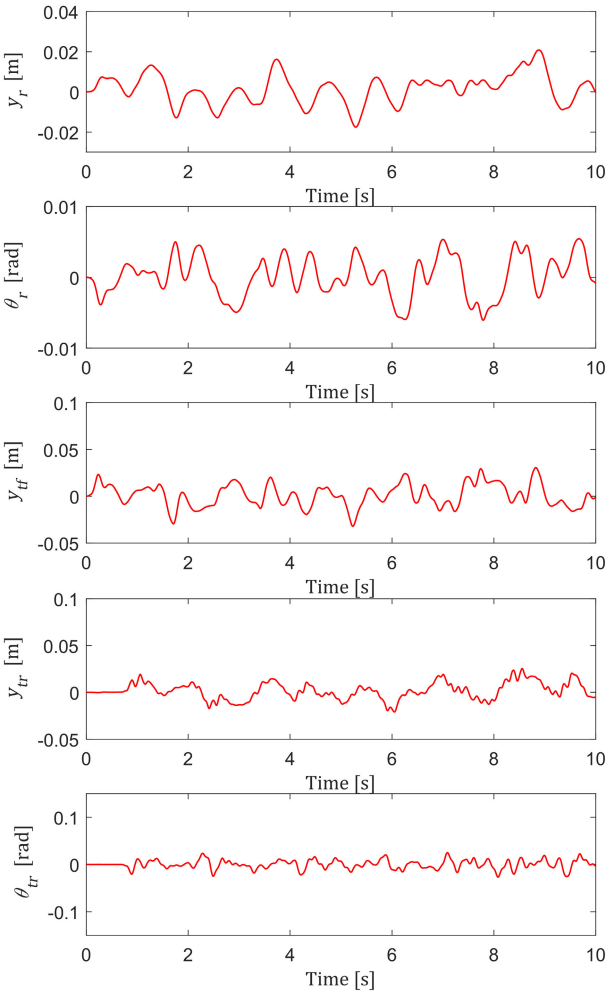

FIGURE 14. Remaining passive states where there is no effect of active control for random road input.

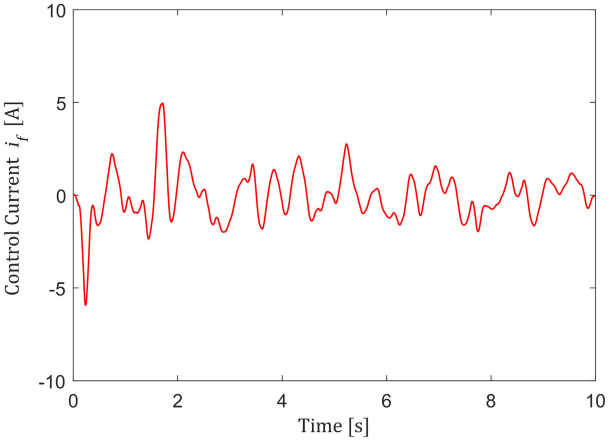

FIGURE 15. Control current for cabin actuator front location.

these time delays and depicted in the figure. While random road input for the front tire starts at time t = 0, it starts after a certain time delay at the rear wheel depending on the speed of the vehicle.

The axial and the angular displacement of the truck cabin's center of mass are given respectively in Fig.12 and Fig.13 for random road profile. In the random road input case, it is observed that the controller significantly suppresses the cabin displacement results. Thereby, the proposed controller significantly reduces the vibrations which cause negative effects on truck drivers and passengers. Similarly, for the 7-DOF truck system's other remaining passive states, where active control effect does not exist, responses to random road profile are given in Fig.14. Lastly, the computed electromagnetic actuator control current inputs for random road input case are given in Fig.15 and Fig.16.

When we compare these figures with the speed bump road input results given in Fig.8 and Fig.9, it can be seen that they do not contain instantaneous peaks, and peaks are located in a relatively narrow interval of ±5 Amperes. Numerical simulation results showed that the active cabin suspension with electromagnetic actuator has good execution in suppression of the vibration than the passive control for both road input cases.

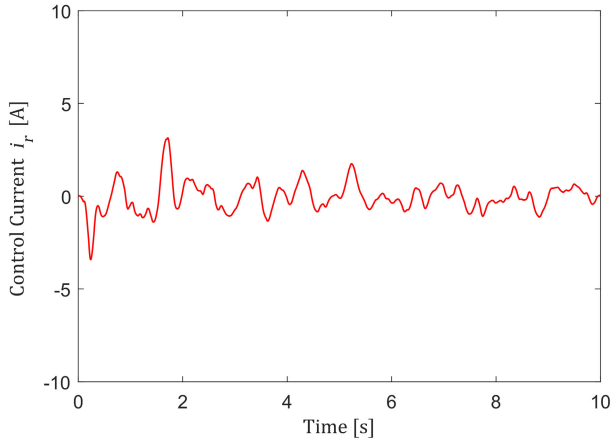

FIGURE 16. Control current for cabin actuator rear location.

V. CONCLUSION

In heavy vehicles like trucks, WBV affecting the driver or passenger are neglected in terms of occupational safety, however, they seriously affect the drivers' performance. In this work, a truck cabin active suspension control design is proposed to eliminate or, at least relieve the problems related to vibration. Lyapunov type vectorial adaptive backstepping control design was realized by considering the electromagnetic actuator dynamics added into the balanced suspension truck system which is modeled with a half-car approach. Road bumps are frequently encountered obstacles in motorways and the designed controller is first applied to a road bump profile, then the simulation repeated for the random road input. Obtained simulation results show that amplitudes of linear and angular displacements are damped. In addition, the usability of electromagnetic actuators in cabin suspension control systems has been demonstrated in this study. Besides, the aforementioned truck model with 7-DOF can be considered for the main suspension system with active control for possible future work.

REFERENCES

[1] J. A. Tamboli and S. G. Joshi, "Optimum design of a passive suspension system af a vehicle subjected to actual random road excitations," *J. Sound Vibrat.*, vol. 219, no. 2, pp. 193–205, Jan. 1999, doi: 10.1006/jsvi.1998.1882.

[2] B. Gadhvi, V. Savsani, and V. Patel, "Multi-objective optimization of vehicle passive suspension system using NSGA-II, SPEA2 and PESA-II," *Procedia Technol.*, vol. 23, pp. 361–368, Jan. 2016, doi: 10.1016/j.protcy.2016.03.038.

[3] A. Florin, M. R. Ioan-Cozmin, and P. Liliana, "Passive suspension modeling using MATLAB, quarter-car model, input signal step type," *New Technol. Products Mach. Manuf. Technol.*, pp. 258–263, Jan. 2013.

[4] J. F. I. Buj, "Integral suspension system for motor vehicles based on passive components," *SAE Trans.*, vol. 111, pp. 761–774, Jan. 2002.

[5] D. Cao, X. Song, and M. Ahmadian, "Editors' perspectives: Road vehicle suspension design, dynamics, and control," *Vehicle Syst. Dyn.*, vol. 49, nos. 1–2, pp. 3–28, Feb. 2011, doi: 10.1080/00423114.2010.532223.

[6] M. M. Elmadany and Z. Abduljabbar, "Design evaluation of advanced suspension systems for truck ride comfort," *Comput. Struct.*, vol. 36, no. 2, pp. 321–331, 1990.

[7] M. Ieluzzi, P. Turco, and M. Montiglio, "Development of a heavy truck semi-active suspension control," *Control Eng. Pract.*, vol. 14, no. 3, pp. 305–312, Mar. 2006, doi: 10.1016/j.conengprac.2005.03.019.

[8] M. Valášek, W. Kortüm, Z. Šika, L. Magdolen, and O. Vaculın, "Development of semi-active road-friendly truck suspensions," *Control Eng. Pract.*, vol. 6, no. 6, pp. 735–744, Jun. 1998, doi: 10.1016/s0967-0661(98)00079-3.

[9] D. E. Ivers and L. R. Miller, "Experimental comparison of passive, semi-active on/off, and semi-active continuous suspensions," SAE Tech. Paper 892484, Nov. 1989, doi: 10.4271/892484.

[10] M. Valášek, M. Novák, Z. Šika, and O. Vaculín, "Extended ground-hook–new concept of semi-active control of Truck's suspension," *Vehicle Syst. Dyn.*, vol. 27, nos. 5–6, pp. 289–303, Jun. 1997, doi: 10.1080/00423119708969333.

[11] D. Fischer and R. Isermann, "Mechatronic semi-active and active vehicle suspensions," *Control Eng. Pract.*, vol. 12, no. 11, pp. 1353–1367, Nov. 2004, doi: 10.1016/j.conengprac.2003.08.003.

[12] G. Z. Yao, F. F. Yap, G. Chen, W. H. Li, and S. H. Yeo, "MR damper and its application for semi-active control of vehicle suspension system," *Mechatronics*, vol. 12, no. 7, pp. 963–973, Sep. 2002.

[13] S.-K. Chung and H. B. Shin, "High-voltage power supply for semi-active suspension system with ER-fluid damper," *IEEE Trans. Veh. Technol.*, vol. 53, no. 1, pp. 206–214, Jan. 2004, doi: 10.1109/tvt.2003.819811.

[14] A. S. Yıldız and S. Sivrioğlu, "Constrained adaptive backstepping control of a semi-active suspension considering suspension travel limits," *Asian J. Control*, early access, doi: 10.1002/asjc.2302.

[15] H. Zhang, J. Liu, E. Wang, S. Rakheja, and C.-Y. Su, "Nonlinear dynamic analysis of a skyhook-based semi-active suspension system with magneto-rheological damper," *IEEE Trans. Veh. Technol.*, vol. 67, no. 11, pp. 10446–10456, Nov. 2018, doi: 10.1109/tvt.2018.2870325.

[16] J. E. D. Ekoru and J. O. Pedro, "Proportional-integral-derivative control of nonlinear half-car electro-hydraulic suspension systems," *J. Zhejiang Univ. Sci. A*, vol. 14, no. 6, pp. 401–416, Jun. 2013, doi: 10.1631/jzus.A1200161.

[17] Q. Wang, Y. Zhao, H. Xu, and Y. Deng, "Adaptive backstepping control with grey signal predictor for nonlinear active suspension system matching mechanical elastic wheel," *Mech. Syst. Signal Process.*, vol. 131, pp. 97–111, Sep. 2019, doi: 10.1016/j.ymssp.2019.05.046.

[18] H. Chen, Z.-Y. Liu, and P.-Y. Sun, "Application of constrained H_∞ control to active suspension systems on half-car models," *J. Dyn. Syst., Meas., Control*, vol. 127, no. 3, pp. 345–354, Oct. 2004, doi: 10.1115/1.1985442.

[19] H. Du, W. Li, and N. Zhang, "Integrated seat and suspension control for a quarter car with driver model," *IEEE Trans. Veh. Technol.*, vol. 61, no. 9, pp. 3893–3908, Nov. 2012, doi: 10.1109/tvt.2012.2212472.

[20] W. Sun, H. Pan, and H. Gao, "Filter-based adaptive vibration control for active vehicle suspensions with electrohydraulic actuators," *IEEE Trans. Veh. Technol.*, vol. 65, no. 6, pp. 4619–4626, Jun. 2016, doi: 10.1109/tvt.2015.2437455.

[21] R. Wang, R. Ding, and L. Chen, "Application of hybrid electromagnetic suspension in vibration energy regeneration and active control," *J. Vibrat. Control*, vol. 24, no. 1, pp. 223–233, Mar. 2016, doi: 10.1177/1077546316637726.

[22] B. L. J. Gysen, T. P. J. van der Sande, J. J. H. Paulides, and E. A. Lomonova, "Efficiency of a regenerative direct-drive electromagnetic active suspension," *IEEE Trans. Veh. Technol.*, vol. 60, no. 4, pp. 1384–1393, May 2011, doi: 10.1109/tvt.2011.2131160.

[23] N. Yagiz, I. Yuksek, and S. Sivrioglu, "Robust control of active suspensions for a full vehicle model using sliding mode control," *JSME Int. J. Ser. C*, vol. 43, no. 2, pp. 253–258, 2000.

[24] H. Pan, X. Jing, W. Sun, and H. Gao, "A bioinspired dynamics-based adaptive tracking control for nonlinear suspension systems," *IEEE Trans. Control Syst. Technol.*, vol. 26, no. 3, pp. 903–914, May 2018, doi: 10.1109/tcst.2017.2699158.

[25] T. Yoshimura, A. Kume, M. Kurimoto, and J. Hino, "Construction of an active suspension system of a quarter car model using the concept of sliding mode control," *J. Sound Vibrat.*, vol. 239, no. 2, pp. 187–199, Jan. 2001, doi: 10.1006/jsvi.2000.3117.

[26] A. G. Thompson, "Design of active suspensions," *Proc. Inst. Mech. Eng.*, vol. 185, no. 1, pp. 553–563, Jun. 1970, doi: 10.1243/pime_proc_1970_185_060_02.

[27] X.-H. Chang, Y. Liu, and M. Shen, "Resilient control design for lateral motion regulation of intelligent vehicle," *IEEE/ASME Trans. Mechatronics*, vol. 24, no. 6, pp. 2488–2497, Dec. 2019, doi: 10.1109/tmech.2019.2946895.

[28] R. Krtolica and D. Hrovat, "Optimal active suspension control based on a half-car model: An analytical solution," *IEEE Trans. Autom. Control*, vol. 37, no. 4, pp. 528–532, Apr. 1992, doi: 10.1109/9.126592.
[29] M. M. ElMadany and Z. S. Abduljabbar, "Linear quadratic Gaussian control of a quarter-car suspension," *Vehicle Syst. Dyn.*, vol. 32, no. 6, pp. 479–497, Dec. 1999, doi: 10.1076/vesd.32.6.479.4224.
[30] K. Jeong, S. B. Choi, and H. Choi, "Sensor fault detection and isolation using a support vector machine for vehicle suspension systems," *IEEE Trans. Veh. Technol.*, vol. 69, no. 4, pp. 3852–3863, Apr. 2020, doi: 10.1109/tvt.2020.2977353.
[31] R. S. Prabakar, C. Sujatha, and S. Narayanan, "Optimal semi-active preview control response of a half car vehicle model with magnetorheological damper," *J. Sound Vibrat.*, vol. 326, nos. 3–5, pp. 400–420, Oct. 2009, doi: 10.1016/j.jsv.2009.05.032.
[32] J. Hwan Jeon, R. V. Cowlagi, S. C. Peters, S. Karaman, E. Frazzoli, P. Tsiotras, and K. Iagnemma, "Optimal motion planning with the half-car dynamical model for autonomous high-speed driving," in *Proc. Amer. Control Conf.*, Jun. 2013, pp. 188–193, doi: 10.1109/acc.2013.6579835.
[33] R. Krtolica and D. Hrovat, "Optimal active suspension control based on a half-car model," in *Proc. 29th IEEE Conf. Decis. Control*, Dec. 1990, pp. 2238–2243.
[34] M. Moradi and A. Fekih, "Adaptive PID-sliding-mode fault-tolerant control approach for vehicle suspension systems subject to actuator faults," *IEEE Trans. Veh. Technol.*, vol. 63, no. 3, pp. 1041–1054, Mar. 2014, doi: 10.1109/tvt.2013.2282956.
[35] A. Kruczek and A. Stribrsky, "A full-car model for active suspension–some practical aspects," in *Proc. IEEE Int. Conf. Mechatronics*, Jun. 2004, pp. 41–45, doi: 10.1109/icmech.2004.1364409.
[36] W. Sun, H. Gao, and B. Yao, "Adaptive robust vibration control of full-car active suspensions with electrohydraulic actuators," *IEEE Trans. Control Syst. Technol.*, vol. 21, no. 6, pp. 2417–2422, Nov. 2013, doi: 10.1109/tcst.2012.2237174.
[37] S. B. Choi, Y. T. Choi, and D. W. Park, "A sliding mode control of a full-car electrorheological suspension system via hardware in-the-loop simulation," *J. Dyn. Syst., Meas., Control*, vol. 122, no. 1, pp. 114–121, Apr. 1998, doi: 10.1115/1.482435.
[38] X. Wang, F. Bi, and H. Du, "Reduction of low frequency vibration of truck driver and seating system through system parameter identification, sensitivity analysis and active control," *Mech. Syst. Signal Process.*, vol. 105, pp. 16–35, May 2018, doi: 10.1016/j.ymssp.2017.12.006.
[39] W. Xiao, D. Lu, L. Song, H. Guo, and Z. Yang, "Influence of particle damping on ride comfort of mining dump truck," *Mech. Syst. Signal Process.*, vol. 136, Feb. 2020, Art. no. 106509, doi: 10.1016/j.ymssp.2019.106509.
[40] D. Ning, S. Sun, H. Du, W. Li, N. Zhang, M. Zheng, and L. Luo, "An electromagnetic variable inertance device for seat suspension vibration control," *Mech. Syst. Signal Process.*, vol. 133, Nov. 2019, Art. no. 106259, doi: 10.1016/j.ymssp.2019.106259.
[41] D. Ning, S. Sun, H. Du, W. Li, and N. Zhang, "Vibration control of an energy regenerative seat suspension with variable external resistance," *Mech. Syst. Signal Process.*, vol. 106, pp. 94–113, Jun. 2018, doi: 10.1016/j.ymssp.2017.12.036.
[42] A. M. A. Soliman, "Improvement of the truck ride comfort via cab suspension," in *Proc. SAE Tech. Paper Ser.*, Apr. 2008, doi: 10.4271/2008-01-1148.
[43] C. Mayhew and M. Quinlan, "Economic pressure, multi-tiered subcontracting and occupational health and safety in australian long-haul trucking," *Employee Relations*, vol. 28, no. 3, pp. 212–229, May 2006, doi: 10.1108/01425450610661216.
[44] R. Nitti and P. De Santis, "Assessment and prediction of whole-body vibration exposure in transport truck drivers," *Ind. Health*, vol. 48, no. 5, pp. 628–637, 2010, doi: 10.2486/indhealth.mswbvi-24.
[45] F. Caffaro, M. M. Cremasco, C. Preti, and E. Cavallo, "Ergonomic analysis of the effects of a telehandler's active suspended cab on whole body vibration level and operator comfort," *Int. J. Ind. Ergonom.*, vol. 53, pp. 19–26, May 2016, doi: 10.1016/j.ergon.2015.10.009.
[46] P. W. Johnson, P. Rynell, and R. Blood, "Differences in whole body vibration exposures between a cab-over and conventional flatbed truck," in *Proc. 3rd Amer. Conf. Human Vibrat.*, 2010, pp. 1–3.
[47] K. Deprez, K. Maertens, and H. Ramon, "Comfort improvement by passive and semi-active hydropneumatic suspension using global optimization technique," in *Proc. Amer. Control Conf.*, May 2002, pp. 1497–1501, doi: 10.1109/acc.2002.1023233.
[48] K. Nakano, "Self-powered active control applied to a truck cab suspension," *JSAE Rev.*, vol. 20, no. 4, pp. 511–516, Oct. 1999.
[49] A. Achen, J. Toscano, R. Marjoram, K. S. Clair, B. Mcmahon, A. Goelz, and S. Shutto, "Semi-active vehicle cab suspension using magnetorheological (MR) technology," *Proc. JFPS Int. Symp. Fluid Power*, vol. 2008, nos. 7–2, pp. 561–564, 2008, doi: 10.5739/isfp.2008.561.
[50] M. M. Elmadany, "Stochastic optimal control of highway tractors with active suspensions," *Vehicle Syst. Dyn.*, vol. 17, no. 4, pp. 193–210, Jan. 1988, doi: 10.1080/00423118808968902.
[51] B. L. J. Gysen, J. J. H. Paulides, J. L. G. Janssen, and E. A. Lomonova, "Active electromagnetic suspension system for improved vehicle dynamics," *IEEE Trans. Veh. Technol.*, vol. 59, no. 3, pp. 1156–1163, Mar. 2010, doi: 10.1109/tvt.2009.2038706.
[52] Z. Gao, S. Chen, Y. Zhao, and Z. Liu, "Numerical evaluation of compatibility between comfort and energy recovery based on energy flow mechanism inside electromagnetic active suspension," *Energy*, vol. 170, pp. 521–536, Mar. 2019, doi: 10.1016/j.energy.2018.12.193.
[53] I. Martins, M. Esteves, F. Pina da Silva, and P. Verdelho, "Electromagnetic hybrid active-passive vehicle suspension system," in *Proc. IEEE 49th Veh. Technol. Conf.*, May 1999, pp. 2273–2277, doi: 10.1109/vetec.1999.778470.
[54] X. Lin, Y. Bo, G. Xuexun, and Y. Jun, "Simulation and performance evaluation of hydraulic transmission electromagnetic energy-regenerative active suspension," in *Proc. 2nd WRI Global Congr. Intell. Syst.*, Dec. 2010, pp. 58–61, doi: 10.1109/gcis.2010.249.
[55] Y. Lu, S. Yang, and S. Li, "Research on dynamics of a class of heavy vehicle-tire-road coupling system," *Sci. China Technolog. Sci.*, vol. 54, no. 8, pp. 2054–2063, Jun. 2011, doi: 10.1007/s11431-011-4490-1.
[56] Y. Chang, Y. Wang, F. E. Alsaadi, and G. Zong, "Adaptive fuzzy output-feedback tracking control for switched stochastic pure-feedback nonlinear systems," *Int. J. Adapt. Control Signal Process.*, vol. 33, no. 10, pp. 1567–1582, Sep. 2019, doi: 10.1002/acs.3052.
[57] L. Ma, N. Xu, X. Huo, and X. Zhao, "Adaptive finite-time output-feedback control design for switched pure-feedback nonlinear systems with average dwell time," *Nonlinear Anal., Hybrid Syst.*, vol. 37, Aug. 2020, Art. no. 100908, doi: 10.1016/j.nahs.2020.100908.
[58] L. Ma, X. Huo, X. Zhao, and G. Zong, "Adaptive fuzzy tracking control for a class of uncertain switched nonlinear systems with multiple constraints: A small-gain approach," *Int. J. Fuzzy Syst.*, vol. 21, no. 8, pp. 2609–2624, Oct. 2019, doi: 10.1007/s40815-019-00708-9.
[59] Y. Ouyang, W. Shi, J. Shan, and B. F. Spencer, "Backstepping adaptive control for real-time hybrid simulation including servo-hydraulic dynamics," *Mech. Syst. Signal Process.*, vol. 130, pp. 732–754, Sep. 2019, doi: 10.1016/j.ymssp.2019.05.042.
[60] H. Pan, H. Li, W. Sun, and Z. Wang, "Adaptive fault-tolerant compensation control and its application to nonlinear suspension systems," *IEEE Trans. Syst., Man, Cybern. Syst.*, vol. 50, no. 5, pp. 1766–1776, May 2020, doi: 10.1109/tsmc.2017.2785796.
[61] Z. Feng, W. Liang, J. Ling, X. Xiao, K. K. Tan, and T. H. Lee, "Integral terminal sliding-mode-based adaptive integral backstepping control for precision motion of a piezoelectric ultrasonic motor," *Mech. Syst. Signal Process.*, vol. 144, Oct. 2020, Art. no. 106856, doi: 10.1016/j.ymssp.2020.106856.
[62] L. Zhang, H. Ding, J. Shi, Y. Huang, H. Chen, K. Guo, and Q. Li, "An adaptive backstepping sliding mode controller to improve vehicle maneuverability and stability via torque vectoring control," *IEEE Trans. Veh. Technol.*, vol. 69, no. 3, pp. 2598–2612, Mar. 2020, doi: 10.1109/tvt.2019.2950219.
[63] J. Yao and W. Deng, "Active disturbance rejection adaptive control of uncertain nonlinear systems: Theory and application," *Nonlinear Dyn.*, vol. 89, no. 3, pp. 1611–1624, May 2017, doi: 10.1007/s11071-017-3538-6.
[64] J. Yao and W. Deng, "Active disturbance rejection adaptive control of hydraulic servo systems," *IEEE Trans. Ind. Electron.*, vol. 64, no. 10, pp. 8023–8032, Oct. 2017, doi: 10.1109/tie.2017.2694382.
[65] T. I. Fossen and S. P. Berge, "Nonlinear vectorial backstepping design for global exponential tracking of marine vessels in the presence of actuator dynamics," in *Proc. 36th IEEE Conf. Decis. Control*, Dec. 1997, pp. 4237–4242, doi: 10.1109/cdc.1997.649499.
[66] Y. Lu, S. Yang, and S. Li, "Heavy vehicle dynamics with balanced suspension based on enveloping tire model," *Frontiers Mech. Eng. China*, vol. 5, no. 4, pp. 476–482, Sep. 2010, doi: 10.1007/s11465-010-0120-z.

[67] M. Krstic, P. V. Kokotovic, and I. Kanellakopoulos, *Nonlinear and Adaptive Control Design*. New York, NY, USA: Wiley, 1995.
[68] M. Čorić, J. Deur, L. Xu, H. E. Tseng, and D. Hrovat, "Optimisation of active suspension control inputs for improved vehicle ride performance," *Vehicle Syst. Dyn.*, vol. 54, no. 7, pp. 1004–1030, May 2016, doi: 10.1080/00423114.2016.1177655.
[69] I. Fialho and G. J. Balas, "Road adaptive active suspension design using linear parameter-varying gain-scheduling," *IEEE Trans. Control Syst. Technol.*, vol. 10, no. 1, pp. 43–54, Aug. 2002, doi: 10.1109/87.974337.
[70] N. Yagiz and Y. Hacioglu, "Backstepping control of a vehicle with active suspensions," *Control Eng. Pract.*, vol. 16, no. 12, pp. 1457–1467, Dec. 2008, doi: 10.1016/j.conengprac.2008.04.003.
[71] X. Zhao, S. Wang, M. Yu, Q. Yu, and C. Zhou, "The position of speed bump in front of truck scale based on vehicle vibration performance," *J. Intell. Fuzzy Syst.*, vol. 34, no. 2, pp. 1083–1095, Feb. 2018, doi: 10.3233/JIFS-169402.
[72] L. He, G. Qin, Y. Zhang, and L. Chen, "Non-stationary random vibration analysis of vehicle with fractional damping," in *Proc. Int. Conf. Intell. Comput. Technol. Autom. (ICICTA)*, Oct. 2008, pp. 150–157, doi: 10.1109/icicta.2008.348.
[73] Z. Yonglin and Z. Jiafan, "Numerical simulation of stochastic road process using white noise filtration," *Mech. Syst. Signal Process.*, vol. 20, no. 2, pp. 363–372, Feb. 2006, doi: 10.1016/j.ymssp.2005.01.009.
[74] Y. Qin, R. Langari, and L. Gu, "The use of vehicle dynamic response to estimate road profile input in time domain," in *Proc. Dyn. Syst. Control Conf.*, Oct. 2014, pp. 1–9, doi: 10.1115/dscc2014-5978.

SINAN BASARAN (Member, IEEE) received the B.S. degree in mechanical engineering from Istanbul Technical University, Istanbul, Turkey, in 2009, the M.S. degree in mechanical engineering from the Gebze Institute of Technology, Kocaeli, Turkey, in 2011, and the Ph.D. degree from Gebze Technical University, Gebze, Turkey, in 2017. He is currently an Assistant Professor with the Department of Mechanical Engineering, Bilecik Seyh Edebali University, Bilecik, Turkey. His research interests include system dynamics and control, magnetic levitation systems, superconducting magnetic bearings, repulsive magnetic bearings, and nonlinear control of mechatronics systems.

MURAT BASARAN received the B.S. degree in electrical and electronics engineering from Eskisehir Osmangazi University, Turkey, in 2005, and the M.S. and Ph.D. degrees in electrical and electronics engineering from Anadolu University, Turkey, in 2009 and 2016, respectively.

He is currently a member of the Department of Motor Vehicles and Transportation Technologies, Vocational School of Transportation, Eskisehir Technical University. His research interests include electric machines, signal processing, and transportation technologies.